Discovery and Selection of TMC114, a Next Generation HIV-1 Protease Inhibitor[§]

Dominique L. N. G. Surleraux,[†] Abdellah Tahri,[†] Wim G. Verschueren,[†] Geert M. E. Pille,[†] Herman A. de Kock,[†] Tim H. M. Jonckers,[†] Anik Peeters,[†] Sandra De Meyer,[†] Hilde Azijn,[†] Rudi Pauwels,[†] Marie-Pierre de Bethune,[†] Nancy M. King,[‡] Moses Prabu-Jeyabalan,[‡] Celia A. Schiffer,[‡] and Piet B. T. P. Wigerinck*[,†]

Tibotec BVBA, Generaal de Wittelaan L 11B 3, B-2800 Mechelen, Belgium, and Department of Biochemistry and Molecular Pharmacology, University of Massachusetts Medical School, Worcester, Massachusetts 01605

Received June 7, 2004

The screening of known HIV-1 protease inhibitors against a panel of multi-drug-resistant viruses revealed the potent activity of TMC126 on drug-resistant mutants. In comparison to amprenavir, the improved affinity of TMC126 is largely the result of one extra hydrogen bond to the backbone of the protein in the P2 pocket. Modification of the substitution pattern on the phenylsulfonamide P2′ substituent of TMC126 created an interesting SAR, with the close analogue TMC114 being found to have a similar antiviral activity against the mutant and the wild-type viruses. X-ray and thermodynamic studies on both wild-type and mutant enzymes showed an extremely high enthalpy driven affinity of TMC114 for HIV-1 protease. In vitro selection of mutants resistant to TMC114 starting from wild-type virus proved to be extremely difficult; this was not the case for other close analogues. Therefore, the extra H-bond to the backbone in the P2 pocket cannot be the only explanation for the interesting antiviral profile of TMC114. Absorption studies in animals indicated that TMC114 has pharmacokinetic properties comparable to currently approved HIV-1 protease inhibitors.

Introduction

The introduction of innovative therapeutic treatments and regimens often changes the impact of disease. For example, with the introduction of HAART[1,2] (Highly Active Anti Retroviral Therapy) AIDS changed, for many patients in the developed world, from a fatal infection into a chronic infectious disease.[3] Following the success of HAART, the key new attributes needed for novel drugs against HIV were those for chronic diseases: safety, tolerability, and ease of administration.[4] However, another unmet medical need has become apparent: resistance and cross-resistance against all available drugs and combinations thereof. Eventually under drug pressure, a virus is selected that harbors a combination of mutations which results in the synthesis of functional viral enzymes with reduced sensitivity to the drugs composing the regimen.

A few years ago we initiated the search for HIV-1 protease inhibitors (PIs) with activity against a broad range of drug-resistant strains. Two evaluation criteria were put forward: (1) high potency on both wild-type and a panel of multi-PI-resistant HIV-1 strains, and (2) favorable pharmacokinetic (PK) properties after oral administration in at least one species. As the complexity of the resistance patterns was already very high, we decided prior to designing new compounds to first profile existing PIs against highly resistant viruses. The rationale behind this was the observation that most teams had been optimizing for wild-type (WT) potency only, and therefore might have discounted compounds with average potency against wild-type which had good potency against resistant strains. A panel of recombinant HIV strains derived from clinical isolates that were highly resistant and cross-resistant to the PIs marketed at that time was selected. The PI-resistance associated mutations[5] present in the selected HIV strains (M1−M5) are shown in Table 1. When comparing compounds for broad-spectrum activity, different methods can be used. A comprehensive method is illustrated in Figure 1. A 2D representation of the data is given: the *X*-axis represents the activity in the cellular antiviral assay on HIV-WT; on the *Y*-axis the average pEC_{50} on the panel of PI-resistant strains is given. A compound with high potency on wild-type (WT) and no activity on these mutants would show up in the right lower corner; a broad spectrum compound (in this panel) will show up

Table 1. PI Resistance-Associated Mutations (ref 5) Present in Panel of Clinical Isolate-Derived Recombinant HIV Strains (M1-M5) Highly Resistant or Cross Resistant to Current PIs[a]

AA in WT	M1	M2	M3	M4	M5
L10	I	M/I	I	L/I	I
K20		R	M		
L24					I
M36		I		I	I
M46	I			L	
I54			V		V
A71	V	V	V	V	V
G73		S			
V77		I			
I84	V	V	V	V	V
N88				D	
L90		M	M	M	

[a] The first column lists the amino acid (AA) present in WT strain for PI resistance-associated mutations and position.

* To whom correspondence should be addressed. Phone: +32 (0)-15292445. Fax: +32(0)15401257. E-mail: pwigeri1@tibbe.jnj.com.

[§] This paper is dedicated to the memory of Dr. Paul Janssen and his commitment to discover new and better drugs in many different disease areas. Dr. Janssen spent the last years of his life together with his multidisciplinary research team focusing on the battle against AIDS.

[†] Tibotec BVBA.

[‡] University of Massachusetts Medical School.

10.1021/jm049560p CCC: $30.25
Published on Web 10/05/2004

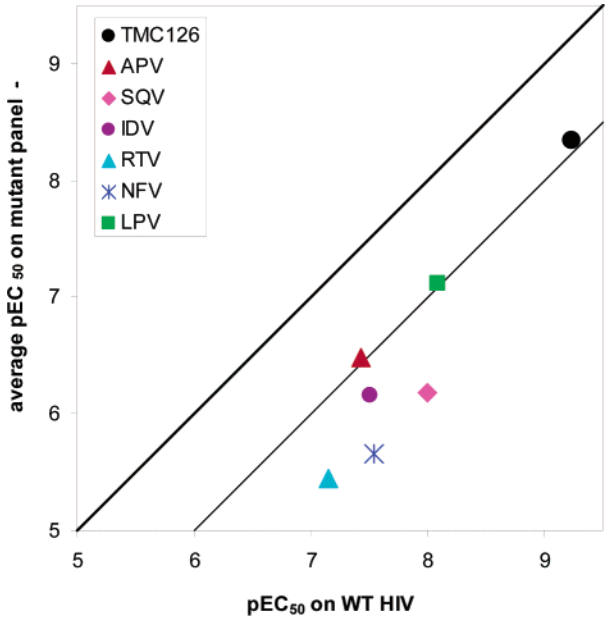

Figure 1. Average activity (expressed as pEC_{50}) on a selected panel of PI-resistant mutants (M1-M5) as a function of the activity against wild-type HIV-1 for currently approved protease inhibitors and compound **1b**.

close to the bisector; a very potent broad spectrum compound will appear in the right upper corner. The further a compound is found below the bisector, the larger the loss in affinity due to the mutations present in the selected panel. Compounds present above the bisector would show hypersensitivity. For the marketed PIs (atazanavir was not assessed), an average difference of >1 log between activity against WT and against the panel of resistant strains is observed. Therefore, most of the compounds are found below the thin line in Figure 1 that represents a 10-fold decreased activity on the mutants with respect to the wild-type virus.

During this search, compound **1b** (TMC126) was tested. Earlier in 1998 the group of Ghosh[6,7] described the compound as a potent, more drug-like inhibitor of HIV-WT. The compound is closely related to amprenavir (APV, **2**), with the tetrahydrofuran (THF) group of **2** replaced by a fused bicyclic tetrahydrofuran moiety and the 4-aminobenzenesulfonamide by a 4-methoxybenzenesulfonamide in the P2′-pocket. The structures of **1b** and **2** are shown in Figure 2. In the selected panel (Table 1) compound **1b** was more active (1.5−2 log) against WT and PI-resistant mutants than the reference drugs, as shown in Figure 1. The compound inhibited all mutants at concentrations lower than the WT EC_{50}s of the currently approved compounds. However, on average the mutants were still 10-fold less sensitive to compound **1b** than the wild-type, a shift comparable to the one observed with **2** and lopinavir (LPV). Moreover, the pharmacokinetic properties of **1b** were found to be insufficient to advance this compound into further development. To improve the pharmacokinetic profile while keeping the high potency, a new series of closely related compounds was synthesized and the data are presented here. These compounds all share the bis-THF moiety for improved interaction in the P2-pocket and differ in the benzenesulfonamide substituent or the stereochemistry of the bis-THF group. One of the compounds in this series, TMC114[8] (**1a**), showed promising broad spectrum activity in combination with promising PK. The binding characteristics of **1a** studied using X-ray and thermodynamic experiments are also presented here.

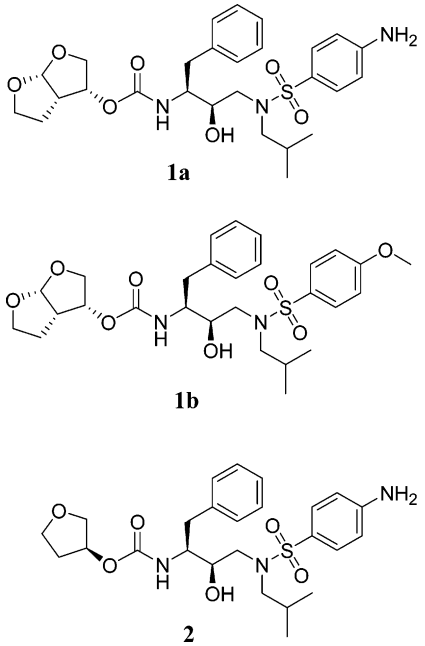

Figure 2. Chemical structure of TMC114 (**1a**), TMC126 (**1b**), and APV (**2**).

Table 2. Overview of the Structure and Preparation Method of the Bis-THF Compounds Included in This Study[a]

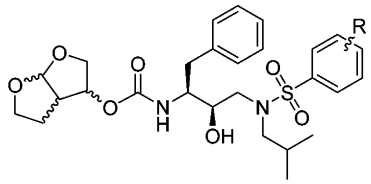

entry	compound	substituent	preparation method	bis-THF stereochemistry
1	**1a** (TMC 114)	4-NH_2	A	3*R*, 3a*S*, 6a*R*
2	**1b** (TMC 126)	4-OCH_3	A	3*R*, 3a*S*, 6a*R*
3	**1c**	3-NH_2	A	3*R*, 3a*S*, 6a*R*
4	**1d**	3,4-OCH_2O-	A	3*R*, 3a*S*, 6a*R*
5	**1e**	4-NH_2	A[b]	3S, 3a*R*, 6a*S*
6	**1f**	4-NH_2	A[b]	3*R*, 3a*R*, 6a*S*
7	**1g**	4-NH_2	A[b]	3S, 3a*S*, 6a*R*
8	**1h**	4-NH_2[c]	from **1l**	3*R*, 3a*S*, 6a*R*
9	**1i**	4-OH	via **4b**	3*R*, 3a*S*, 6a*R*
10	**1j**	4-CN	B	3*R*, 3a*S*, 6a*R*
11	**1k**	4-CH_2NH_2	from **1j**	3*R*, 3a*S*, 6a*R*
12	**1l**	4-NO_2	B	3*R*, 3a*S*, 6a*R*
13	**1m**	4-I	B	3*R*, 3a*S*, 6a*R*
14	**1n**	4-CO-CH_3	B	3*R*, 3a*S*, 6a*R*
15	**1o**	4-CH_3	B	rac[d]
16	**1p**	4-H	B	rac[d]

[a] The structures differ only in the substituent present in the P2′-pocket (column 3) and the stereochemistry of the bis-THF moiety (column 5). [b] Prepared as presented in Scheme 3. [c] Ca-phosphate derivative. [d] rac indicates a racemic activated bis-THF mixture was used.

Chemistry

The general synthetic route we applied for the synthesis of protease inhibitors **1a**−**p** (Table 2) is outlined in Schemes 1−4. In general, two different approaches were followed. Method A (Scheme 1) starts from 3-dibenzylamino-1-isobutylamino-4-phenylbutan-2-ol (**3**)[9] which

Scheme 1. Synthesis of {1-Benzyl-2-hydroxy-3-[(R-benzenesulfonyl)isobutylamino]propyl}carbamic Acid Hexahydrofuro[2,3-*b*]furan-3-yl Ester Derivatives **1a**−**d** and **1i** Using Method A[a]

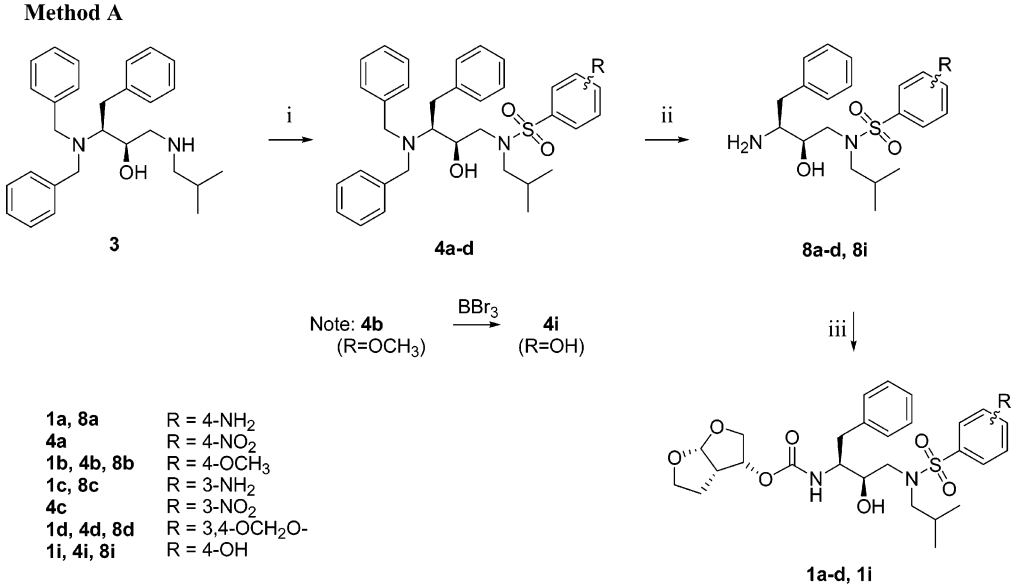

[a] (i) R-phenyl-SO_2Cl, Et_3N, CH_2Cl_2; (ii) Pd/C, H_2 MeOH; (iii) **11a**, Et_3N, THF.

Scheme 2. Synthesis of a Second Set of {1-Benzyl-2-hydroxy-3-[(R-benzenesulfonyl)isobutylamino]propyl}carbamic Acid Hexahydrofuro[2,3-*b*]furan-3-yl Ester Derivatives **1j**, **1l**−**p** Using Method B[a]

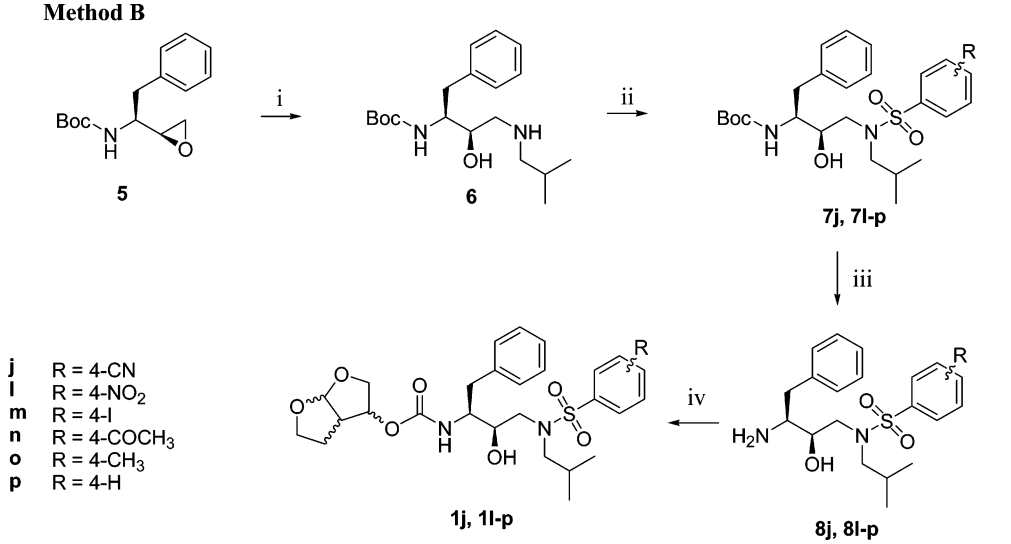

[a] (i) Isobutylamine, CH_2Cl_2; (ii) R-phenyl-SO_2Cl, Et_3N, CH_2Cl_2; (iii) HCl/*i*-PrOH; (iv) **11a, 11e**−**g**, Et_3N, THF.

was reacted with substituted phenylsulfonyl chlorides yielding sulfonamides **4a**−**d**. Compound **4i** was obtained through demethylation of **4b** with BBr_3 in CH_2Cl_2. Debenzylation of these compounds yielded free amino alcohols **8a**−**d** and **8i**. It has to be emphasized that in the case of **4a** and **4c**, debenzylation is accompanied with reduction of the nitro group yielding the corresponding amino derivatives. Then, target compounds **1a**−**d** and **1i** were obtained through reaction with carbonic acid 2,5-dioxopyrrolidin-1-yl ester hexahydrofuro[2,3-*b*]furan-3-yl ester **11a**. The synthesis of this intermediate and some of its stereoisomers is discussed below. The reaction with the 3*R*,3a*S*,6a*R*-enantiomer **11a** is preferred, as this results in the optimal conformation for backbone interactions in the P2-pocket of the enzyme.

The second method (method B) starts from commercially available (1-oxiranyl-2-phenylethyl)carbamic acid *tert*-butyl ester **5** (Scheme 2), which was reacted with isobutylamine thereby forming the amino alcohol **6.**[10] Similar as in method A, reaction with another set of substituted sulfonyl chlorides yielded sulfonylamides **7j**, **7l**−**p** which were deprotected to give amino alcohols **8j**, **8l**−**p** which were finally transformed into target compounds **1j**, **1l**−**p**.

In addition to the compounds described above, some target compounds were obtained by standard functional group transformations. For instance, compound **1k** was obtained by reduction of the nitril group of **1j**. Furthermore, with the possible benefits of prodrugs in mind, the Ca^{2+}-phosphate salt of **1a** was also prepared (**1h**). While Methods A and B can be regarded as the two general approaches for the synthesis of all protease inhibitors, some comment is needed regarding the synthesis of analogues of **TMC114** (**1a**) with different stereochemistry in the bis-THF moiety.[11] As will be

Scheme 3. Synthesis of Enantiomerically Pure "Bis-THF-alcohols" and Their Transformation into the Corresponding Activated Carbonates[a]

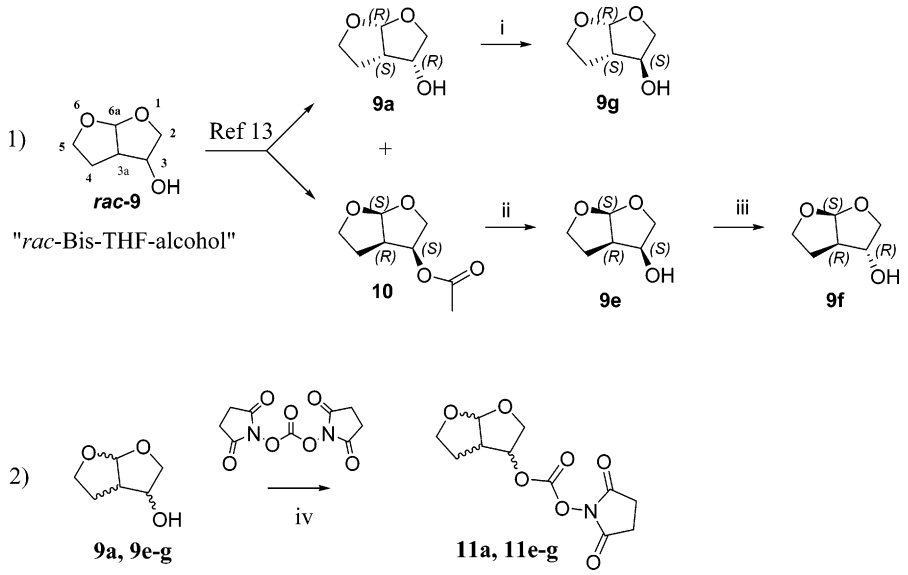

[a] (i) (1) DIAD, PPh_3, CH_3COOH, (2) K_2CO_3, EtOH; (ii) K_2CO_3, EtOH; (iii) (1) DIAD, PPh_3, CH_3COOH, (2) K_2CO_3, EtOH; (iv) Et_3N, CH_2Cl_2.

Scheme 4. Synthesis of **1a** and Some Stereoisomers[a]

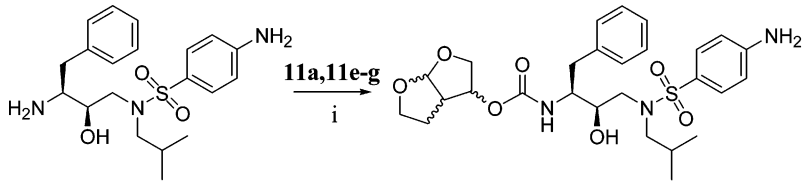

1a	(3*R*,3a*S*, 6a*R*)	**TMC114**
1e	(3*S*,3a*R*, 6a*S*)	
1f	(3*R*,3a*R*, 6a*S*)	
1g	(3*S*,3a*S*, 6a*R*)	

[a] (i) Et_3N, CH_2Cl_2.

illustrated below, the exact stereochemistry of this element of the molecule is of paramount importance for the resulting biological activity.

The synthesis and rationale behind the design of this bis-THF moiety was already reported by Ghosh et al.[12] in 1994. Initially a synthetic strategy starting from optically pure diethyl malates was reported which was later replaced by a cobaloxime-mediated radical cyclization methodology yielding *rac*-**9**.[13] In addition, the enzymatic resolution of this racemate using immobilized Lipase 30 was reported also, which resulted in "bis-THF"-alcohol **9a** and acetylated derivative **10**. Scheme 3 illustrates this pioneering work which was further extended by us using Mitsunobu chemistry. This resulted in the synthesis of stereoisomers **9a** and **9e**−**g**, which were all transformed into the corresponding enantiomerically pure carbonic acid 2,5-dioxo-pyrrolidin-1-yl ester hexahydrofuro[2,3-*b*]furan-3-yl esters **11a** and **11e**−**g** by reaction with *N*,*N*′-disuccinimidyl carbonate.[14]

With these enantiomeric pure compounds in hand, we were able to complete the synthesis of **1a**-stereoisomers **1e**, **1f**, and **1g** by reaction of 4-amino-*N*-(3-amino-2-hydroxy-4-phenylbutyl)-*N*-isobutylbenzenesulfonamide (**8a**) with the activated carbonates **11a** and **11e**−**g** (Scheme 4).

Results and Discussion

Structure−**Activity Relationships.** In the search for new potent HIV-1 protease inhibitors, one of the most important criteria for the next-generation compounds is an improved activity against a broad range of drug-resistant HIV strains. As shown in Figure 1, the PIs currently on the market cannot be considered as having a broad spectrum because their average activity against a panel of resistant mutants is more than 1 log lower than their wild-type activity. For the bis-THF compounds listed in Table 2, a similar plot was constructed (Figure 3). When compared to Figure 1, all compounds in Figure 3 show an improved activity against both wild-type and mutant virus strains. As a reference the best marketed compound from Figure 1, LPV, has also been included in Figure 3. This compound showed an activity similar to the weakest member of the bis-THF family. The antiviral activity of the bis-THF compounds on each of the selected mutant strains is presented in Table 3. From these data it can be seen that the average activity as presented in Table 3 and Figure 3 is in most cases the result of a larger decrease in activity for M1 and M2 and a smaller effect for mutants M3−M5. For some compounds, e.g. **1a** and **1k**, the largest decrease in pEC_{50} value observed, 0.25 and

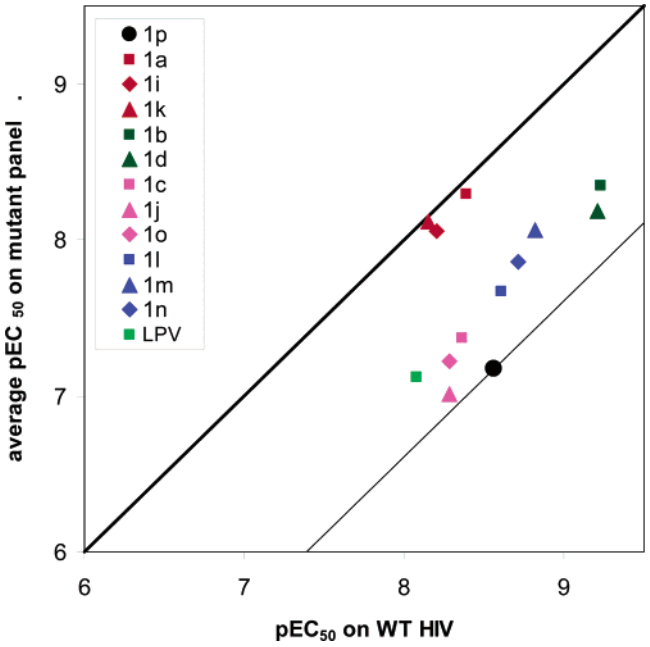

Figure 3. Average activity (expressed as pEC_{50}) on selected panel of PI-resistant mutants (M1-M5) as a function of the activity against wild-type HIV-1 for the bis-THF compounds presented in this paper. Lopinavir has been included as a reference.

Table 3. Antiviral Activity against Wild Type (IIIB) and PI-Resistant Strains M1−M5, and Average Activity on the Mutant Panel (AVMUT), Expressed as pEC_{50}[a]

	IIIB	M1	M2	M3	M4	M5	AVMUT
1a	8.39	8.29	8.14	8.4	8.41	8.22	8.29
1b	9.23	7.99	8.22	8.65	8.33	8.54	8.35
1c	8.36	6.82	7.32	7.55	7.58	7.58	7.37
1d	9.21	7.49	8.19	8.46	8.4	8.39	8.19
1e	7.97	7.43	7.22	7.67	7.67	7.58	7.51
1f	6.51						
1g	6.62	6.12	5.65	6.32	5.95		6.01
1h	7.36		6.72	6.76	6.84	6.9	6.81
1i	8.2	7.63	8	8.22	8.22	8.21	8.06
1j	8.28	6.94	6.81	7.4	7.05	6.86	7.01
1k	8.15	8.12	7.8	8.22	8.18	8.25	8.11
1l	8.61	7.47	7.53	8.34	7.66	7.34	7.67
1m	8.82	7.48	7.86	8.39	8.28	8.3	8.06
1n	8.71	7.5	7.78	8.22		7.93	7.86
1o	8.28	6.89	6.97	7.45	7.42	7.39	7.22
1p	8.56	6.78	6.87	7.32	7.38	7.51	7.17
2	7.43	6.13	6.69	6.71	6.77	6.13	6.49

[a] Data are included for the bis-THF compounds and **2**.

0.35, respectively, is even smaller than the difference of 0.5 log that is considered to be significant in these assays. For the averaged values presented on the *Y*-axis, the significance level drops down to 0.25 log.

A detailed SAR of different substituents introduced on the P2′-phenyl group can be derived starting from the unsubstituted phenyl compound (**1p**), presented as a black dot in Figure 3. The bis-THF compounds have been grouped according to their activities, both on WT and on the small panel of mutants, and all compounds within one group are presented in Figure 3 using the same color-code. Introduction of a *p*-CN (**1j**), *p*-CH_3 (**1o**), or *m*-NH_2 (**1c**) substituent (shown in pink in Figure 3) hardly influences the antiviral characteristics of the compounds on both the wild-type and the mutant viruses. Introduction of a *p*-nitro (**1l**), *p*-acetyl (**1n**), and especially a *p*-iodo (**1m**) substituent (all electron-withdrawing substituents, shown as blue markers) does not influence the potency on the WT-virus but significantly increases the activity on the mutant viruses. For the *p*-OCH_3 (**1b**) and the 3,4-dioxolane (**1d**) derivatives (small electron-donating and H-bond-accepting groups), the activity on the mutants is even higher than for the previous group. In addition, these compounds also show a higher activity on the WT virus when compared to the unsubstituted compound **1p**. In fact, these compounds (**1b** and **1d**, shown in green in Figure 3) have the highest activity on wild-type virus of all the compounds presented here ($pEC_{50} > 9$). Unfortunately, their activity on the mutants is still about 1 log less than on the wild-type virus. In Figure 3, one group of compounds (shown in red) with wild-type activity comparable to **1p** is found very close to the bisector and can therefore be considered as potent broad spectrum inhibitors of the selected panel. This group contains the *p*-NH_2 (**1a**), *p*-OH (**1i**), and *p*-CH_2NH_2 (**1k**) substituents: small, polar, and with both hydrogen bond-donating and -accepting capability. They are the only compounds as active on the WT as on this panel of mutants. An X-ray structure of the complex of HIV-1 protease with the *p*-NH_2 derivative indicates that this substituent forms a hydrogen bond with the backbone C=O of Asp30′ and another water-mediated hydrogen bond with the side chain of Asp30′ in the P2′-pocket. Modeling has shown that also the *p*-OH and *p*-CH_2NH_2 substituents can pick up at least one of these interactions. In addition, the backbone NH of Asp30′ is also within reach of a hydrogen bond-accepting group substituted on the benzene ring. The N···H−N distance in the *p*-NH_2 X-ray structure is 2.53 Å. This interaction with N−H (Asp30′) is also present in the compounds with the highest activity on WT enzyme, **1b** and **1d**, and because of the nature of the substituents in this group, the lone pairs are oriented differently and the interaction tends to be stronger than it is in the case of the red group. This type of interaction seems to be more important for interacting with the WT enzyme, resulting in a shift of approximately 1 log value from the weak interacting (red) to the strong interacting (green) group of compounds. This shift already indicates the importance of the position of the hydrogen acceptor and the orientation of the lone pairs. The position of the O-atom in **1b** might also be influenced by the presence of van der Waals interactions of the methyl group with side chains present in the P2′-pocket. In the case of mutations of these side chains, the orientation and position of the methyl group might be altered, resulting in a less optimal orientation of the oxygen lone pair toward the NH (Asp30′) and a drop in activity. The compounds that are found close to the bisector interact primarily as hydrogen bond donors rather than hydrogen acceptor. They can donate a hydrogen bond to Asp30′ in many different ways (by interacting with the backbone or the flexible side chain or both) and are therefore less susceptible to changes in the structure of the enzyme. This explains why these compounds also remain active on the mutants in the selected panel.

The importance of the interactions in the P2-pocket at the other side of the active site is obvious when comparing **1a** with **2**, two compounds that differ only in the functional group present in this pocket. The

Table 4. Hydrogen Bonds Present in the P2-Pocket of the Active Site. Distances Are in Angstroms

	2	**1a**
(Asp29) N−H···O(THF-2)	-	1.96
(Asp30) N−H···O(THF-1)	2.11	2.08
(Asp29) N−H···O(THF-1)	2.36	2.43

Table 5. Binding Thermodynamics Derived from Isothermal Titration Calorimetry for **1a**, **1b**, and **2** at 20 °C

	K_a (M^{-1})	K_d (M)	ΔH (kcal/mol)	$-T\Delta S$ (kcal/mol)	ΔG (kcal/mol)
		L63P/V82T/I84V[a]			
2	5.1×10^8	2.0×10^{-9}	−7.0	−4.7	−11.7
1a	1.7×10^{10}	6.0×10^{-11}	−10.0	−3.7	−13.7
		V82F/I84V[b]			
2	4.8×10^7	2.1×10^{-8}	−3.9	−6.6	−10.5
1b	2.3×10^{10}	4.4×10^{-11}	−9.6	−4.5	−14.1

[a] Reference 10. [b] Reference 11.

activity (pEC_{50}) measured on HIV-WT in a AVE-MT4-MTT cell-line is 8.39 for **1a**, while it is 7.43 for **2**. Recently, both compounds have been crystallized with a multi-drug-resistant mutant of the enzyme (L63P, V82T, I84V).[15] The crystals for both structures were obtained under similar experimental conditions. The structures crystallized in the space group $P2_12_12_1$, with similar cell dimensions and one dimer per asymmetric unit. Data for the **1a** structure were collected at −80 °C using a synchrotron source, while data for **2** were collected at room temperature on a rotating anode source. The crystal structure with **1a** diffracted to a resolution of 1.35 Å, with an *R*-factor of 16.8%. For the complex with **2**, a resolution of 2.2 Å was obtained. Despite the different ways of data collection, these X-ray structures form an ideal basis for the comparison of compounds **1a** and **2**. Hydrogen atoms have been added to the structures, and the position of these atoms has been optimized using InsightII. For these all-atom structures, the intermolecular interactions in the P2-pocket of the enzyme are tabulated in Table 4. The O-atom of the tetrahydrofuran moiety of **2** forms a strong hydrogen bond to the backbone N−H of Asp30. In the case of **1a**, an additional hydrogen bond with the backbone of Asp29 is formed by the second tetrahydrofuran ring in **1a**. In addition, this second ring is also in a favorable position for interaction with the side chain of Asp29. The interactions with Asp29 account for a 10-fold increase in activity for compound **1a** when compared to **2**. Similar conclusions were drawn in a recent paper by Tie et al.[16] on the X-ray structures of **1a** in complex with wild-type and two single mutant HIV-1 proteases.

The thermodynamic data derived from isothermal titration calorimetry[15] as shown in Table 5 also support these findings. In this experiment the binding thermodynamics of the compounds to the same multi-drug-resistant mutant (L63P, V82T, I84V) have been measured. The binding free enthalpy for **1a** is 3 kcal/mol larger than for **2**, which may be in part due to the additional hydrogen bond interaction. The association constant K_a observed for **1a** (1.7×10^{10} M^{-1}) is also in line with the observation by Ohtaka et al.[17] on the closely related compound TMC126 (**1b**) for a double mutant (V82F/I84V). Related studies for first generation inhibitors indinavir (IDV), ritonavir (RTV), saquinavir (SQV), and nelfinavir (NFV) have shown that the binding of these inhibitors to HIV-1 protease is mainly entropy-driven,[18] whereas binding of **2** is both enthalpically and entropically driven. In the case of **1a** and **1b**, the enthalpic contribution seems to be the dominant one as a consequence of the tight interactions between these compounds and the enzyme. This high affinity due to backbone interactions is only one of the reasons why these compounds retain their wild-type potency also against multi-drug-resistant viruses. Another reason is the fact that **1a** and **1b**, as well as **2**, lie predominantly within the so-called substrate envelope. This substrate envelope is defined as the consensus volume, i.e., the region occupied by the natural substrates of the enzyme.[19,20] It is known that all first generation inhibitors do not fit well into this envelope. In addition, it has been shown that the primary drug-resistant mutations often occur at positions in the protease that are contacted by inhibitor atoms protruding beyond the volume of the substrate envelope.[21] This observation explains why **2**, **1a**, and **1b** have a different pattern of selecting viral mutants and drug resistance compared to first generation inhibitors.

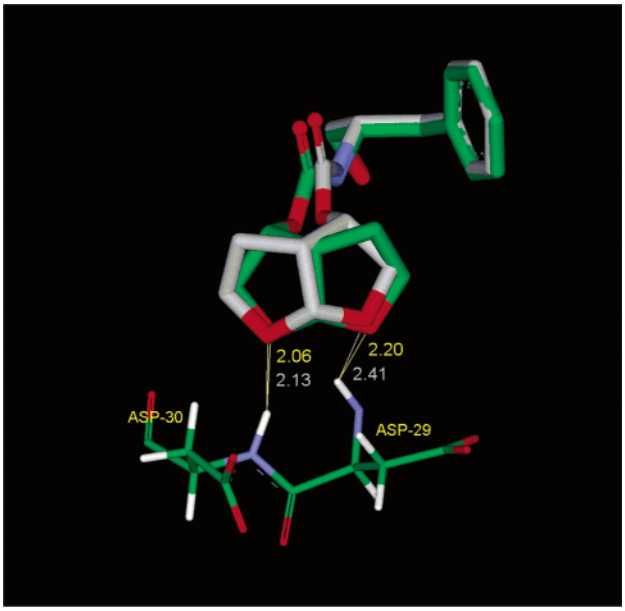

Figure 4. Superposition of compounds **1a** (C-atoms colored in green) and **1e** (C-atoms colored in gray). For simplicity, only a part of the structures is shown. The strongest hydrogen bond interactions with amino acids Asp 29 and Asp 30 are indicated in yellow for compound **1a** and in gray for **1e**.

It is also interesting to link the activity of the different bis-THF isomers **1a**, **1e**, **1f**, and **1g** to their interactions in the P2-pocket. The most important interactions present in this pocket are backbone interactions with the N−H groups of Asp29 and Asp30. In compound **2**, containing only one THF ring, only the interaction with Asp30 is present. This compound has a $pEC_{50} = 7.43$ on the wild-type enzyme. In compound **1a**, the additional interaction with Asp29 accounts for a 10-fold increase in the activity ($pEC_{50} = 8.39$). Modeling has indicated that compound **1e** is also able to interact with both Asp29 and Asp30. This is illustrated in Figure 4. The figure presents a superposition of compounds **1a** and **1e** in the P2-pocket. Please note that in order to interact with the 2 backbone N−H groups, compound

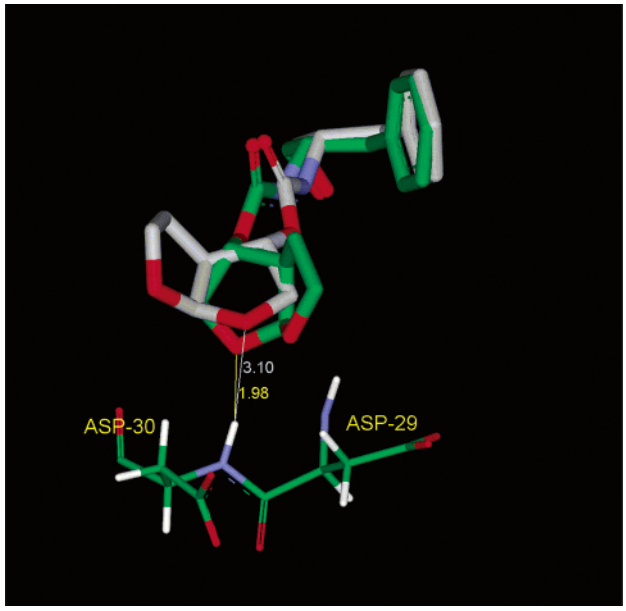

Figure 5. Superposition of compounds **1f** (C-atoms colored in green) and **1g** (C-atoms colored in gray). For simplicity, only a part of the structures is shown. The interaction with amino acid Asp 30 is indicated in yellow for compound **1f** and in gray for **1g**.

1e needs to adopt a conformation in which the carbamate group is in a different position than it is in the case of compound **1a**. This might be the reason for the observed decrease in the activity against HIV-WT for **1e** (pEC_{50} of **1e** = 7.97). The average activity on the mutants is approximately 0.5 log lower than the HIV-WT activity for compound **1e**, whereas it is almost the same for **1a**. In Figure 5 a superposition of the two remaining stereoisomers, **1f** and **1g**, is shown. Both isomers are able to interact with the backbone of Asp30 in a similar way as **2** interacts with the enzyme, although in the case of the **1g** model this is a very weak hydrogen bond. As can be seen from Figure 5, the second ring of the bis-THF system in **1f** and **1g** is found in a sterically unfavorable position, and therefore the activity of stereoisomers **1f** and **1g** is lower than the activity of **2**.

In Vitro Selection Experiments. The results presented above suggest different pathways for the development of resistance for some of the described compounds as compared to currently approved PIs. To investigate this, in vitro selection experiments were conducted, where cells infected with WT virus were exposed to increasing concentrations of the inhibitors and the emerging virus populations were characterized genotypically and phenotypically. The results of these experiments are presented in Figure 6. In this figure, both **2** and RTV are included as references. Data have been normalized, i.e., the fold-increase in selecting concentration (rather than the absolute concentration of the inhibitors) is plotted against time. In the lab, within 100 days of in vitro culture in the presence of a suboptimal concentration ($3 \times EC_{50}$) of **2** or RTV, a virus is selected that is 100 times less sensitive to the inhibitor and that carries the same mutations as the ones observed in patients on a failing PI-containing therapy. **1b** and **1d** behaved in the same way; i.e., within 100 days, a virus carrying known PI-resistance

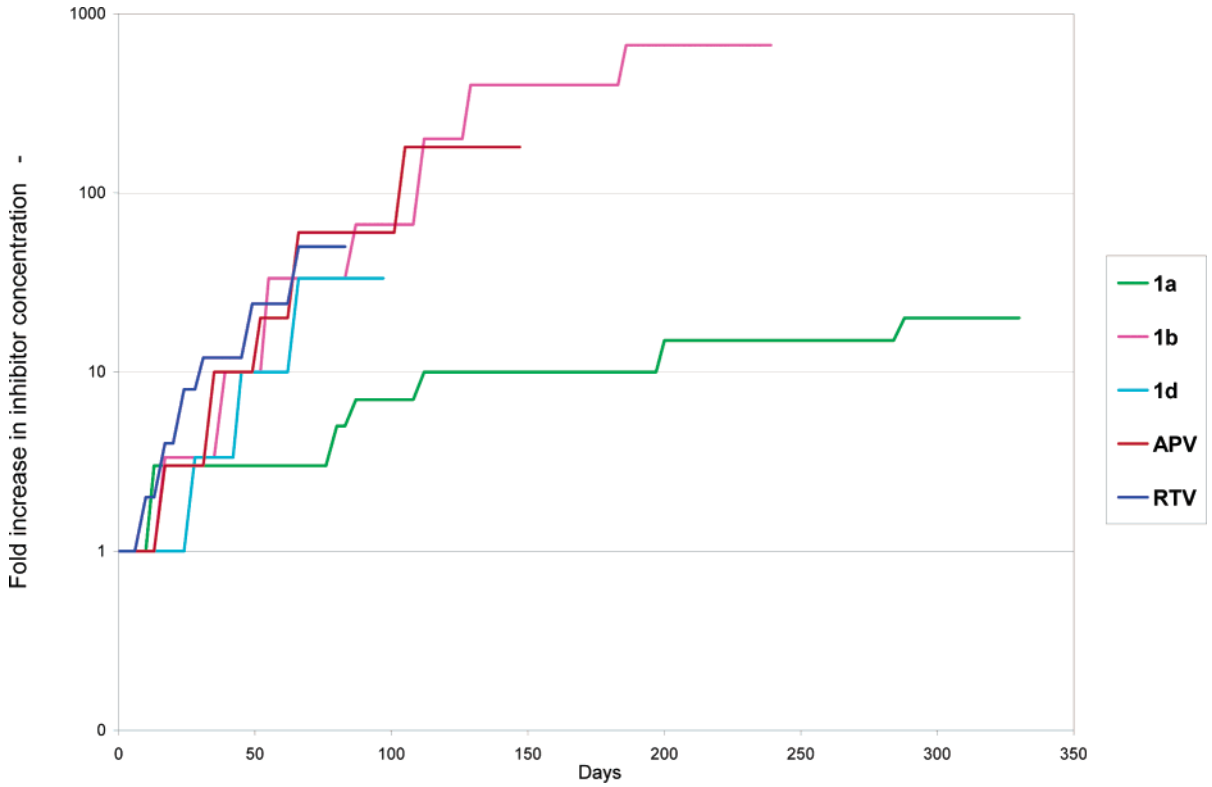

Figure 6. Results of in vitro selection experiments for compounds **1a**, **1b**, **1d**, **2**, and RTV. Cells infected with WT virus were exposed to increasing concentrations of the inhibitors (see Experimental Section). Data have been normalized, i.e., the fold-increase in inhibitor concentration (rather than the absolute concentration of the inhibitors) is plotted against time. This is obtained by the ratio of the inhibitor concentration at time *t* and the inhibitor concentration at the start of the selection experiments.

Table 6. Metabolic Stability in Three Different Species as % Remaining Parent Compound after 30 min Incubation with Liver Microsomes of Rat, Dog, and Human Origin

compound	rat	dog	human
1a	92	80	85
1b	25	11	56
1d	21	53	52
2	83	81	116
IDV	97	85	95

Table 7. PK Data after Oral Administration in Dog and Rat

compound	C_{max} (ng/mL)	T_{max} (h)	AUC_{last} (ng h/mL)	$T_{1/2}$ (h)
		Dog[a]		
1a	19100 (± 5919)	1.0 (± 0.4)	74081 (± 39355)	0.7812 (± 0.1994)
1b	1181 (± 750)	0.6 (± 0.3)	2695 (± 1972)	1.4743 (± 0.6766)
1d	3778 (± 639)	2.5 (± 1.0)	18111 (± 3906)	2.0583 (± 0.5296)
		Rat[b]		
1a	998.5	1.0	1578.5	2.06
1h	712	0.5	1474	6.04

[a] Data in dog generated for **1a**, **1b**, and **1d** at 80 mg/kg are presented as the mean values of four measurements. The value between parentheses represents the standard deviation [b] Data after oral administration at 20 mg/kg in rat have been generated for **1a** and **1h**. The values reported are the average of two measurements.

associated mutations and with a 100-fold reduced sensitivity was selected. **1a** (TMC114) performed differently; even after 1 year, the sensitivity for **1a** is only reduced by a factor of 20, and moreover the mutations appearing are not those observed in patients failing PI therapy.[22] The viruses that were isolated in the presence of **1a** remained sensitive to most of the current PIs.

Pharmacokinetics. The second selection criterion was a set of pharmacokinetic related properties. In Table 6 the metabolic stability is presented in three different species (liver microsomes of rat, dog, and human origin) as % remaining parent compound after 30 min incubation at 37 °C. The degree of metabolism is determined by direct measurement of the residual parent compound in the reaction mixture using LC-MS. **1b** and **1d** appeared to be extremely labile. **1a** had a stability comparable to other protease inhibitors. **2** and IDV have been included as a reference in Table 6.

The same trend was observed in oral absorption studies in animals. Data of oral administration to dogs at 80 mg/kg as a PEG400 solution are presented in Table 7. **1a** is clearly superior to **1b** and **1d** both in terms of C_{max} and AUC. During this evaluation, for compound **1b** only minor levels of possible metabolite **1i** were observed. In analogy with fosamprenavir, the monophosphate prodrug of **2**, we studied the behavior of compound **1h**, the monophosphate ester of **1a**. The main advantage of this type of prodrugs are their superior solid-state characteristics, which is outside the scope of this publication. We only investigated the potential for higher bioavailability. Data of a single oral administration in PEG400 in rats at 20 mg/kg were generated; the parent compound and the monophosphate behave in a similar way. For **2** and its prodrug, similar observations were reported previously.[23]

Conclusions

Screening against a panel of PI-resistant mutant HIV strains allowed us to identify a promising class of protease inhibitors with activity against both wild-type and a broad range of PI-resistant HIV strains. Close analogues of the lead compound showed different types of antiviral properties both in terms of spectrum and in vitro selection of resistant viruses. The broad spectrum activity of **1a** is due to both the bis-THF ring interacting in the P2-pocket and the primary aniline group on the sulfonamide part present in the P2′-pocket.

TMC114 was selected for clinical development based on its high potency against both wild-type HIV and PI-resistant mutants, together with a very slow emergence of resistant viruses in vitro, and superior pharmacokinetic properties. TMC114 is currently in phase IIB (dose-finding) clinical trials.

Experimental Section

Chemistry. General Experimental Procedures. NMR spectra were recorded on a Bruker Avance 400 spectrometer, operating at 400 MHz for ^1H and 100 MHz for ^{13}C and with DMSO as solvent unless otherwise stated. In every case tetramethylsilane (TMS) was used as internal standard. Chemical shifts are given in ppm and *J* values in Hz. Multiplicity is indicated using the following abbreviations: d for doublet, t for a triplet, m for a multiplet, etc. Low-resolution mass spectra (LRMS) were performed on a single quadrupole (Waters ZMD), ion trap (ThermoFinnigan LCQ Deca) or a time-of-flight (Waters LCT) mass spectrometer using electrospray ionization (ESI) in positive or negative mode. All reagents were purchased from commercial sources (Acros, Aldrich, etc.) and were used as received. Column chromatography was carried out on silica gel 60 Å, 60−200 μm (ROCC). Thin-layer chromatography was performed on silica gel 60 F_{254} plates (Merck). Optical rotations were measured at the sodium D line, using a Propol-automatic polarimeter. Analytical HPLC was done on a Waters Alliance 2690 (pump + auto sampler) system equipped with a Waters 996 photodiode array-detector. To check the purity of the end products (**1a**−**p**), two independent chromatographic systems were used. First system: column: Waters Xterra MS C18, (3.5 μm, 4.60 mm × 100 mm), mobile phase A: 10 mM CH_3COONH_4 in H_2O, mobile phase B: CH_3CN. Analysis were run at 30 °C using a flow rate of 1 mL/min applying the following gradient: 0 min: 5%B, 10 min: 95%B, 12 min: 95%B. In every case, 10 μL of a 1 mM solution was injected. The equilibration time between two runs was 3 min. Second system (polar): column: Alltech Prevail C18 (3.0 μm, 4.6 mm × 100 mm), mobile phase A: 10 mM CH_3COONH_4 in H_2O, mobile phase B: CH_3CN. Analysis were run at 30 °C using a flow rate of 1 mL/min applying the following gradient: 0 min: 0%B, 1 min: 0%B, 9 min: 95%B, 12 min: 95%B. In every case, 10 μL of a 1 mM solution was injected. The equilibration time between two runs was 3 min. Eluted peaks were detected at a single wavelength (λ_{max}) for both systems. The retention time for each compound is given for both systems and is reported in minutes. GC analysis was performed on a HP5890 gas chromatograph equipped with an on column injector using a DB-XLB column (length: 15 m, I.D.: 0.25 mm, film: 0.25 μm). The detection was done with a flame ionization detector operating at a temperature of 370 °C. Volumes of 0.1 μL were injected, the carrier gas used was helium, and runs were performed operating at pressure of 75 kPa. The temperature gradient applied was 30 °C/min. In those cases were GC data are given, retention time is reported in minutes.

***N*-(3-Dibenzylamino-2-hydroxy-4-phenylbutyl)-*N*-isobutyl-4-nitrobenzenesulfonamide (4a).** To a stirred solution of 3-dibenzylamino-1-isobutylamino-4-phenylbutan-2-ol (**3**) (12.5 g, 30.0 mmol) in dry CH_2Cl_2 (200 mL) was added Et_3N (3.34 g, 33.0 mmol, 1.1 equiv) followed by 4-nitrobenzenesulfonyl chloride (6.98 g, 31.5 mmol, 1.05 equiv). The mixture was stirred at ambient temperature for 4 h after which it was washed twice with 200 mL of H_2O. The organic layer was dried on $MgSO_4$, filtered, and evaporated to dryness. The crude product was then recrystallized from 2-propanol, yielding **4a**

(14.31 g, 23.78 mmol, 79%) after filtering and drying. $C_{34}H_{39}N_3O_5S$, LRMS(ES+): *m/z* 602 $(M + H)^+$.

4-Amino-*N*-(3-amino-2-hydroxy-4-phenylbutyl)-*N*-isobutylbenzenesulfonamide (8a). A solution of **4a** (20 g, 33.2 mmol) and Pd/C (2 g) in 100 mL of MeOH was stirred at ambient temperature and hydrogenated until the starting material had disappeared as judged by TLC and LC-MS. The mixture was filtered over dicalite and evaporated to dryness. Pure compound was obtained by recrystallization from 2-propanol. After drying, **8a** (12.4 g, 31.7 mmol, 95%) was obtained as an off-white solid. $C_{20}H_{29}N_3O_3S$, LRMS(ES+): *m/z* 392 $(M + H)^+$; ^{1}H NMR ($CDCl_3$): δ(ppm): 0.87 (d, $J = 6.61$, 3H, CH_3 (isobutyl)), 0.93 (d, $J = 6.61$, 3H, CH_3 (isobutyl)), 1.87 (m, 1H, CH (isobutyl)), 2.47(dd, $J = 13.49$, $J = 9.92$, 1H, H4a), 2.81 (dd, $J = 13.36$, $J = 6.70$, 1H, CH−N (isobutyl)), 2.96 (dd, 1H, $J = 13.61$, $J = 3.82$, 1H, H4b), 3.01 (dd, 1H, $J = 13.37$, $J = 8.41$, CH−N (isobutyl)), 3.11 (m, 1H, NH_2, H3), 3.15 (dd, $J = 15.21$, $J = 2.54$, 1H, H1a), 3.29 (dd, 1H, $J = 15.04$ and $J = 8.43$, 1H, H1b), 3.72 (ddd, 1H, $J = 8.94$, $J = 4.91$ Hz, $J = 2.72$, 1H, H2), 4.15 (br s, 2H, NH_2), 6.68 (d, 2H, $J = 8.75$, CH (aromatic)), 7.16−7.35 (m, 5H, CH (phenyl)), 7.58 (d, 2H, $J = 8.74$, CH (aromatic)). ^{13}C NMR ($CDCl_3$): δ(ppm): 19.92 (CH_3), 20.20 (CH_3), 27.20 (CH), 39.3 (CH_2), 52.68 (CH_2), 55.73 (CH), 58.66 (CH_2), 73.26 (CH), 114.10 (CH), 126.42 (CH), 126.73 (C), 128.59 (CH), 129.28 (CH), 129.51 (CH), 138.80 (C), 150.56 (C−SO_2).

(3*R*,3a*S*,6a*R*)-{3-[(4-Aminobenzenesulfonyl)isobutylamino]-1-benzyl-2-hydroxypropyl}carbamic Acid Hexahydrofuro[2,3-*b*]furan-3-yl Ester (1a, TMC114). A solution of **8a** (1 g, 2.55 mmol), Et_3N (0.516 g, 5.1 mmol, 2 equiv), and carbonic acid 2,5-dioxopyrrolidin-1-yl ester hexahydrofuro[2,3-*b*]furan-3-yl ester (**11a**)[13] (0.80 g, 2.94 mmol, 1.15 equiv) in 20 mL of CH_2Cl_2 was stirred at ambient temperature until TLC and LC-MS indicated completion of the reaction. Volatiles were evaporated, and the compound was purified by column chromatography using CH_2Cl_2/MeOH 98/2 as the eluent. After evaporation, **1a** (1.26 g, 2.30 mmol, 90%) was obtained as a white solid. $C_{27}H_{37}N_3O_7S$, LRMS(ES+): *m/z* 548 $(M + H)^+$; ^{1}H NMR ($CDCl_3$): δ(ppm): 0.88 (d, $J = 6.6$, 3H, CH_3), 0.92 (d, $J = 6.6$, 3H, $-CH_3$), 1.3−1.37 (m, 1H), 1.5−1.6 (m, 1H), 1.7−1.75 (m, 1H), 2.75−2.99 (m, 7H), 3.67−3.73 (m, 3H), 3.83−3.87 (m, 4H), 4.21 (br s, 2H, NH_2), 4.9−5.0 (m, 2H), 5.63 (d, $J = 5.2$, 1H, H6a), 6.68 (d, $J = 8.64$, 2H), 7.18−7.2 (m, 5H), 7.5 (d, $J = 8.64$, 2H). ^{13}C NMR ($CDCl_3$): δ(ppm): 20.3 (CH_3), 20.5 (CH_3), 26.2 (CH_2), 27.6 (CH), 36.0 (CH_2), 45.8 (CH), 54.09 (CHN), 59.2 (CH_2), 70.0 (CH), 71.2 (CH_2), 73.2 (CH), 73.7 (CH), 109.7 (CH), 114.5 (CH), 126.2 (C), 126.9 (CH), 128.8 (CH), 129.7 (CH), 129.88 (CH), 138.19 (=C−N), 151.36 (C−SO_2), 155.88 (CO). Purity: system 1: $t_R = 7.48$ min: 99.44%, system 2: $t_R = 8.00$ min: 98.79%.

Virology. Cells and Viruses. MT-4 cells are human T-lymphoblastoid cells that are highly sensitive to HIV infection, producing a rapid and strong cytopathic effect. MT4-LTR-EGFP cells are MT4 cells stably transfected with a vector containing the coding sequence for the Green Fluorescent Protein (EGFP) under control of HIV-1 Long Terminal Repeat (LTR). Upon infection of these cells with HIV, the viral transactivator protein Tat activates the LTR promoter, which in turn triggers the transcription of the EGFP coding sequence. All cells were cultured in RPMI 1640 medium supplemented with fetal calf serum and antibiotics in a humidified incubator with a 5% CO_2 atmosphere at 37 °C.

HIV strains used for the profiling of the compounds were wild-type HIV-1 strain IIIB and recombinant HIV strains derived from clinical isolates. Those were constructed as previously described[24] by cotransfection of MT-4 cells with sample-derived viral protease (PR) and reverse transcriptase (RT) coding sequences and an HIV-1 HXB2-derived proviral clone deleted in the protease and RT coding region.

Antiviral Assays. The antiviral activity of compounds against wild-type HIV and clinical sample derived recombinant viruses was determined using the 3-(4,5-dimethylthiazol-2-yl)-2,5-diphenyltetrazolium bromide (MTT) colorimetric assay method as previously described.[25] Briefly, various concentrations of the test compounds were added to wells of a flat-bottom microtiter plate. Subsequently, virus and MT-4 cells were added to a final concentration of 200−250 50% cell culture infectious doses ($CCID_{50}$)/well and 30 000 cells/well, respectively. After 5 days of incubation at 37 °C with 5% CO_2, the cytopathic effect (CPE) of the replicating virus was measured by the MTT method.

The results of the antiviral assay were expressed as pEC_{50} ($= -\log EC_{50}$), with EC_{50} defined as the concentration of a compound achieving 50% CPE compared with the drug-free control. Cytotoxicity of the test compound was determined in parallel using mock-infected cell cultures containing an identical compound concentration range but no virus.

Genotyping. Genotypic analysis was performed by automated population-based full-sequence analysis (ABI PRISM BigDye Terminator cycle sequencing). Sequencing results are reported as amino acid changes compared to the wild-type (HXB2) reference sequence.[26]

In Vitro Selection of Resistant Strains. MT-4-LTR-EGFP cells were infected at a multiplicity of infection of 0.01 to 0.001 $CCID_{50}$/cell in the presence of the inhibitor compound at a starting concentration two to three times the EC_{50}. The cultures were subcultivated and scored microscopically on virus-induced fluorescence and cytopathic effect every 3 to 4 days. Cultures were subcultivated in the presence of the same concentration of compound until full virus breakthrough, and subsequently at a higher compound concentration to select for variants able to grow in the presence of the highest possible inhibitor concentration.

X-ray Crystallography. A multi-drug-resistant HIV-1 protease with substitutions L63P, V82T, and I84V was crystallized in complex with **1a** and **2**. Both structures crystallized in the space group $P2_12_12_1$ with one dimer per asymmetric unit. Data on the **1a** complex were collected under cryocooled conditions using the synchrotron source at Advanced Light Source at Lawrence-Berkeley Laboratory, Berkeley, CA. The crystal complex with **1a** diffracted to a resolution of 1.35 Å, with an *R*-factor of 16.8%. Data for the complex with **2** were collected at room temperature on an R-axis IV image plate system mounted on a Rigaku rotating anode source. The resolution obtained for the complex with **2** is 2.2 Å. The details of the X-ray crystallography experiments and the refinement statistics have been published elsewhere.[15] The X-ray structures have been submitted to the Protein Data Bank (PDB-codes 1T7I and 1T7J).

Isothermal Titration Calorimetry. Thermodynamic parameters of inhibitor binding were determined using an isothermal titration calorimeter, VP-ITC (MicroCal Inc., Northampton, MA). The buffer used for all protease and inhibitor solutions consisted of 10 mM sodium acetate pH 5.0, 2% DMSO, and 2 mM tris(2-carboxyethyl)phosphine (TCEP). The binding affinities of **2** and **1a** for the multi-drug-resistant protease were obtained by the displacement titration method, using acetyl-pepstatin and indinavir, respectively, as the weaker binder.[17,27,28] Direct titration experiments were also performed with the tightly binding inhibitor to confirm the enthalpy changes obtained by the displacement method. Each experiment was performed at least twice. The details of the ITC experiments have been published elsewhere.[15]

Modeling. The structures obtained after X-ray crystallography have some missing and disordered side chains and do not contain information on the position of the hydrogen atoms. Therefore, the structures were first completed using the Biopolymer module in InsightII (Accelrys Inc). This was followed by an optimization of the hydrogen atoms using the conjugate gradient approach. The CVFF force field[29] was used in the Discover module of InsightII to perform these optimizations. The refinement was finished when the largest derivative was smaller than 0.01.

For the comparison of the stereoisomers of **1a**, the stereochemistry of the bis-THF moiety in the X-ray structure of **1a** was adapted in order to obtain the correct stereochemistry of compounds **1e**, **1f**, and **1g**. Subsequently, the geometry of the active site was optimized for all four stereoisomers. The active

site was defined as the region of the complex containing the compound and the amino acids having at least one atom closer than 6 Å to any atom of the compound. The optimization was performed using the CVFF force-field[29] in Discover (InsightII) using the conjugate gradient approach until the largest derivative was smaller than 0.01. After the refinement, the resulting structures were superimposed, and the superposition of the bis-THF parts of the closest analogues is presented in Figures 4 and 5. These figures have been generated using DS ViewerPro 5.0 (Accelrys Inc).

Acknowledgment. M.P., N.M.K., and C.A.S. were supported by the National Institutes of Health P01-GM66524 and Tibotec/COSAT.

Supporting Information Available: Experimental details for the synthetic procedures and characterization data for intermediate and final compounds. This material is available free of charge via the Internet at http://pubs.acs.org.

References

(1) Bartlett, J. A.; DeMasi, R.; Quinn, J.; Moxham, C.; Rousseau, F. Overview of the effectiveness of triple combination therapy in antiretroviral-naive HIV-1 infected adults. *AIDS* **2001**, *15*, 1369−1377.

(2) Gulick, R. M.; Mellors, J. W.; Havlir, D.; Eron, J. J.; Meibohm, A.; Condra, J. H.; Valentine, F. T.; McMahon, D.; Gonzalez, C.; Jonas, L.; Emini, E. A.; Chodakewitz, J. A.; Isaacs, R.; Richman, D. D. 3-year suppression of HIV viremia with indinavir, zidovudine, and lamivudine. *Ann. Intern. Med.* **2000**, *133*, 35−39.

(3) Palella, F. J.; Delaney, K. M.; Moorman, A. C.; Loveless, M. O.; Fuhrer, J.; Satten, G. A.; Aschman, D. J.; Holmberg, S. D. 1998. Declining morbidity and mortality among patients with advanced human immunodeficiency virus infection. HIV Outpatient Study Investigators. *N. Engl. J. Med.* **1998**, *338*, 853−860.

(4) d'Arminio, M. A.; Lepri, A. C.; Rezza, G.; Pezzotti, P.; Antinori, A.; Phillips, A. N.; Angarano, G.; Colangeli, V.; De Luca, A.; Ippolito, G.; Caggese, L.; Soscia, F.; Filice, G.; Gritti, F.; Narciso, P.; Tirelli, U.; Moroni, M. Insights into the reasons for discontinuation of the first highly active antiretroviral therapy (HAART) regimen in a cohort of antiretroviral naive patients. I.CO.N.A. Study Group. Italian Cohort of Antiretroviral-Naive Patients. *AIDS* **2000**, *14*, 499−507.

(5) D'Aquila, R. T. Drug resistance mutations in HIV. *Top. HIV Med.* **2003**, *11*, 92−96.

(6) Ghosh, A. K.; Kincaid, J. F.; Cho, W.; Walters, D. E.; Krishnan, K.; Hussain, K. A.; Koo, Y.; Cho, H.; Rudall, C.; Holland, L.; Buthod, J. Potent HIV protease inhibitors incorporating high-affinity P2-ligands and (R)−(hydroxyethylamino)sulfonamide isostere. *Bioorg. Med. Chem. Lett.* **1998**, *8*, 687−90.

(7) Yoshimura, K.; Kato, R.; Kavlick, M. F.; Nguyen, A.; Maroun, V.; Maeda, K.; Hussain, K. A.; Ghosh, A. K.; Gulnik, S. V.; Erickson, J. W.; Mitsuya, H. A potent human immunodeficiency virus type 1 protease inhibitor, UIC-94003 (TMC-126), and selection of a novel (A28S) mutation in the protease active site. *J. Virol.* **2002**, *76*, 1349−1358.

(8) Koh, Y.; Nakata, H.; Maeda, K.; Ogata, H.; Bilcer, G.; Devasamudram, T.; Kincaid, J. F.; Boross, P.; Wang, Y.-F.; Tie, Y.; Volarath, P.; Gaddis, L.; Harrison, R. W.; Weber, I. T.; Ghosh, A. K.; Mitsuya, H. Novel bis-tetrahydrofuranylurethane-containing nonpeptidic protease inhibitor (PI) UIC-94017 (TMC114) with potent activity against multi-PI-resistant human immunodeficiency virus in vitro. *Antimicrob. Agents Chemother.* **2003**, *47*, 3123−3129.

(9) Liu, C.; Ng, J. S.; Behling, J. R.; Yen, C. H.; Campbell, A. L.; Fuzail, K. S.; Yonan, E. E.; Mehrotra, D. V. Development of a Large-Scale Process for an HIV Protease Inhibitor. *Org. Process Res. Dev.* **1997**, *1*, 45−54.

(10) Ng, J. S.; Przybyla, C. A.; Zhang, S. Method of preparing retroviral protease inhibitor intermediates via diastereomer purification. PCT Int. Appl. 1996, WO 9622275.

(11) Although the correct nomenclature of this moiety according to IUPAC rules is hexahydrofuro[2,3-*b*]furan-3-yl, we opted, for the sake of clarity, to name this structural entity "bis-THF".

(12) Ghosh, A. K.; Thompson, W. J.; Fitzgerald, P. M. D.; Culberson, C.; Axel, M. G.; McKee, S. P.; Huff, J. R.; Anderson, P. S. Structure-Based Design of HIV-1 Protease inhibitors: Replacement of Two Amides and a 10π-Aromatic System by a Fused Bis-tetrahydrofuran. *J. Med. Chem.* **1994**, *37*, 2506−2508.

(13) Ghosh, A. K.; Chen, Y. Synthesis and Optical Resolution of High Affinity P_2-ligands for HIV-1 protease Inhibitors. *Tetrahedron Lett.* **1995**, *36*, 505−508.

(14) (a) Erickson, J. W.; Gulnik, S. V.; Ghosh, A. K.; Hussain, K. A. Multidrug-resistant retroviral protease inhibitors and associated methods. PCT Int. Appl. 1999, WO 9967254. (b) Ghosh, A. K.; Bilcer, G. M.; Devasamudram, T. Preparation of carbamates as HIV protease inhibitors. PCT Int. WO 2003078438, 2003.

(15) King, N. M.; Prabu-Jeyabalan, M.; Nalivaika, E. A.; Wigerinck, P.; de Béthune, M.-P.; Schiffer, C. A. The structural and thermodynamic basis for the binding of TMC114, a next-generation HIV-1 protease inhibitor. *J. Virol.*, in press.

(16) Tie, Y.; Boross, P. I.; Wang, Y. F.; Gaddis, L.; Hussain, A. K.; Leshchenko, S.; Ghosh, A. K.; Louis, J. M.; Harrison, R. W.; Weber, I. T. High-resolution crystal structures of HIV-1 protease with a potent non-peptide inhibitor (UIC-94017) active against multi-drug-resistant clinical strains. *J. Mol. Biol.* **2004**, *338*, 341−352.

(17) Ohtaka, H.; Velazquez-Campoy, A,; Xie, D.; Freire, E. Overcoming drug resistance in HIV-1 chemotherapy: the binding thermodynamics of Amprenavir and TMC-126 to wild-type and drug-resistant mutants of the HIV-1 protease. *Protein Sci.* **2002**, *11*, 1908−1916.

(18) Todd, M. J.; Luque, I.; Velazquez-Campoy, A.; Freire, E. Thermodynamic basis of resistance to HIV-1 protease inhibition: calorimetric analysis of the V82F/I84V active site resistant mutant. *Biochemistry* **2000**, *39*, 11876−11883.

(19) Prabu-Jeyabalan, M.; Nalivaika, E. A.; Schiffer, C. A. Substrate shape determines specificity of recognition for HIV-1 protease: Analysis of crystal structures of six substrate complexes. *Structure* **2002**, *10*, 369−381.

(20) Prabu-Jeyabalan, M.; Nalivaika, E. A.; King, N. M.; Schiffer, C. A. Viability of a drug-resistant HIV-1 protease variant: structural insights for better anti-viral therapy. *J. Virol.* **2003**, *77*, 1306−1315.

(21) Schiffer, C. A. In preparation

(22) De Meyer, S.; Azijn, H.; Van Ginderen, M.; De Baere, I.; Pauwels, R.; de Béthune M.-P. Presented at the XIth International HIV Drug Resistance Workshop, Seville, Spain, 2002.

(23) Furfine, E. S.; Baker, C. T.; Hale, M. R.; Reynolds, D. J.; Salisbury, J. A.; Searle, A. D.; Studenberg, S. D.; Todd, D.; Tung, R. D.; Spaltenstein, A. Preclinical pharmacology and pharmacokinetics of GW433908, a water-soluble prodrug of the human immunodeficiency virus protease inhibitor amprenavir. *Antimicrob. Agents Chemother.* **2004**, *48*, 791−798.

(24) Hertogs, K.; de Bethune, M. P.; Miller, V.; Ivens, T.; Schel, P.; Van Cauwenberge, A.; Van Den Eynde, C.; Van Gerwen, V.; Azijn, H.; Van Houtte, M.; Peeters, F.; Staszewski, S.; Conant, M.; Bloor, S.; Kemp, S.; Larder, B.; Pauwels, R. A rapid method for simultaneous detection of phenotypic resistance to inhibitors of protease and reverse transciptase in recombinant human immunodeficiency virus type 1 isolates from patients treated with antiretroviral drugs. *Antimicrob. Agents Chemother.* **1998**, *42*, 269−276.

(25) Pauwels, R.; Balzarini, J.; Baba, M.; Snoeck, R.; Schols, D.; Herdewijn, P.; Desmyter, J.; De Clercq, E. Rapid and automated tetrazolium-based colorimetric assay for the detection of anti-HIV compounds. *J. Virol. Methods* **1988**, *20*, 309−321.

(26) Larder, B. A.; Kohli, A.; Kellam, P.; Kemp, S. D.; Kronick, M.; Henfrey, R. D. Quantitative detection of HIV-1 drug resistance mutations by automated DNA sequencing. *Nature* **1993**, *365*, 671−673.

(27) Sigurskjold, B. Exact analysis of competition ligand binding by displacement isothermal titration calorimetry. *Anal. Biochem.* **2000**, *277*, 260−266.

(28) Velazquez-Campoy, A.; Kiso, Y.; Freire, E. The binding energetics of first- and second-generation HIV-1 protease inhibitors: implications for drug design. *Arch. Biochem. Biophys.* **2001**, *390*, 169−175.

(29) Dauber-Osguthorpe, P.; Roberts, V. A.; Osguthorpe, D. J.; Wolff, J.; Genest, M.; Hagler, A. T. Structure and energetics of ligand binding to proteins: E. coli dihydrofolate reductase- trimethoprim, a drug-receptor system. *Proteins: Struct., Funct. Genet.* **1988**, *4*, 31−47.

JM049560P